

Article

Aldol Condensation of Cyclohexanone and Furfural in Fixed-Bed Reactor

Zdeněk Tišler , Pavla Vondrová, Kateřina Hrachovcová , Kamil Štěpánek, Romana Velvarská, Jaroslav Kocík and Eliška Svobodová * 

Unipetrol Centre of Research and Education, a.s, Areál Chempark 2838, Záluží 1, 436 70 Litvínov, Czech Republic; zdenek.tisler@unicre.cz (Z.T.); pavla.vondrova@unicre.cz (P.V.); Katerina.Hrachovcova@unicre.cz (K.H.); kamil.stepanek@unicre.cz (K.Š.); romana.velvarska@unicre.cz (R.V.); jaroslav.kocik@unicre.cz (J.K.)

* Correspondence: eliska.svobodova@unicre.cz

Received: 15 November 2019; Accepted: 12 December 2019; Published: 14 December 2019



Abstract: Aldol condensation reaction is usually catalysed using homogeneous catalysts. However, the heterogeneous catalysis offers interesting advantages and the possibility of cleaner biofuels production. Nowadays, one of the most used kinds of heterogeneous catalysts are hydrotalcites, which belong to a group of layered double hydroxides. This paper describes the aldol condensation of cyclohexanone (CH) and furfural (F) using Mg/Al mixed oxides and rehydrated mixed oxides in order to compare the catalyst activity after calcination and rehydration, as well as the possibility of its regeneration. The catalysts were synthesized by calcination and subsequent rehydration of the laboratory-prepared and commercial hydrotalcites, with Mg:Al molar ratio of 3:1. Their structural and chemical properties were determined by several analytical methods (inductively coupled plasma analysis (ICP), X-ray diffraction (XRD), diffuse reflectance infrared Fourier transform spectroscopy (DRIFT), specific surface area (BET), thermogravimetric analysis (TGA), temperature programmed desorption (TPD)). F-CH aldol condensation was performed in a continuous fixed-bed reactor at 80 °C, CH:F = 5:1, WHSV 2 h⁻¹. The rehydrated laboratory-prepared catalysts showed a 100% furfural conversion for more than 55 h, in contrast to the calcined ones (only 24 h). The yield of condensation products FCH and F2CH was up to 68% and 10%, respectively. Obtained results suggest that Mg/Al mixed oxides-based heterogeneous catalyst is suitable for use in the aldol condensation reaction of furfural and cyclohexanone in a fixed-bed reactor, which is an interesting alternative way to obtain biofuels from renewable sources.

Keywords: Mg/Al hydrotalcite; Mg/Al mixed oxide; aldol condensation; cyclohexanone; furfural

1. Introduction

Because of the increasing environmental awareness and dwindling supplies of fossil resources as a traditional feedstock, new alternative methods to obtain chemical compounds and fuels are recently given significant research attention [1]. Moreover, the substitution of fossil fuels from renewable resources has been proposed in the European Union as a part of the strategy to eliminate greenhouse gas emissions from the transport. The main goal of these efforts is to lower environmental impacts of the traditional methods such as CO₂ production, air pollution, etc., and to develop sustainable methods of maximum utilization of the alternative biomass resources. It is also important to avoid competition with food production. Because of its availability and socio-economic acceptability, the attention is paid mostly to lignocellulose-rich biomass [2–5].

One of the alternative ways to obtain fuels from renewable resources is cyclohexanone condensation reaction. This reaction of organic synthesis is known as a tool for producing complex molecules. Aldol condensation proceeds in the presence of a catalyst, either acidic or basic. During the condensation,

C–C bonds are generated between precursor molecules of relatively simple organic compounds that are typical intermediates in biomass processing [6]. Furfural (F) and cyclohexanone (CH) are suitable model compounds for aldol condensation. The reaction between them is an efficient way to produce ketones with 11 or 16 carbon atoms, which are usable for fuels synthesis [7]. Furfural often denoted as a platform compound in chemical synthesis, and both furfural and cyclohexanone can be obtained from biomass. Specifically, furfural can be obtained via acid hydrolysis of sugar cane residue after processing and subsequent extraction. Cyclohexanone can be obtained from lignin and represents an alternative cyclic biomass platform compound which is considered as an ideal feedstock for high-density aviation fuel synthesis [8–10].

Aldol condensation is usually catalysed using homogeneous catalysts, for example NaOH, KOH, Ca(OH)₂, Na₂CO₃, etc. Heterogeneous catalysis, unlike so far mostly used homogeneous catalysis, brings advantages, such as higher selectivity, easier catalyst recovery, elimination of wastewater streams and by-products, that would contribute to pollution of the environment. Heterogeneous catalysts offer a possibility of cleaner biofuels production, as well as the possibility to replace commonly used batch reactors with continuous fixed-bed reactors [11,12]. All that taking into account, significant research attention is given to heterogeneous catalysis nowadays. Some examples of heterogeneous catalysts that are currently in use are single metal oxides, doped and mixed metal oxides, metal hydroxides, metal complexes, supported catalysts (e.g., alumina-supported), zeolites and hydrotalcites [13].

Hydrotalcites (HTC) have been reported to be promising heterogeneous catalysts and have been successfully used for aldol condensation reactions [7,14–18]. HTCs, from the group of layered double hydroxides (LDH), are solid materials of natural or synthetic origin, which have a brucite-like structure. The structure consists of [Mg(OH)₂] layers in which Mg²⁺ ions are substituted by trivalent M³⁺ cations, for example Al and the excess positive charge is compensated by anions (mostly CO₃²⁻, NO₃⁻) located in the interlayer space along with water molecules. After calcination, the layered structure collapses and Mg/Al mixed oxide is formed, and then rehydration results in the exchange of anions for OH⁻ and the formation of strongly basic Brønsted centres [14,19–22].

Main objectives of this study is to evaluate properties of heterogeneous catalyst based on laboratory prepared and commercial hydrotalcites and to compare their characteristics according to the evaluation of the obtained data. In the present work, we have studied aldol condensation of cyclohexanone and furfural over Mg/Al mixed oxides with molar ratio of Mg/Al = 3:1, calcined at 450 °C in the continuous flow fixed-bed reactor. Our results suggest that investigated Mg/Al mixed oxides-based heterogeneous catalysts are suitable for the aldol condensation reaction, considering their relatively low costs, high activity and stability at high temperatures as well as in aqueous solution. Potential disadvantage could be their sensitivity to CO₂, which significantly reduces their activity. Overall, it is a promising alternative way to obtain biofuels from renewable resources.

2. Results and Discussion

2.1. Structure of Precursors and Catalysts

Laboratory prepared sample of Mg/Al hydrotalcite had a higher molar ratio than target ratio of 3:1, precisely 3.45:1 (25 wt.% of Mg to 8 wt.% of Al). This can be due to the using nitrate hydrates for the synthesis, in which the amount of bonded water molecules can vary. In case of the commercial sample, there was lower Mg/Al ratio than declared 3:1, precisely 2.15:1 (21.4 wt.% of Mg to 11 wt.% of Al), probably caused by alumina addition as an additive of the extrusion process.

Diffuse reflectance infrared Fourier transform spectroscopy (DRIFT) analysis of the hydrotalcite samples shows the differences between laboratory prepared and commercial hydrotalcites before and after rehydration and calcination (Figure 1a). DRIFT spectra were very similar to other results reported in previous research works [15,23–27]. The typical broad band around 3000–3600 cm⁻¹ was attributed to the stretching vibrations of hydroxyl groups in the brucite-like layers. The band around 1640 cm⁻¹ was ascribed to the presence of water molecules. The bands around 1360–1420 cm⁻¹ showed

the presence of carbonate anions in the intralayer and the band at 1510 cm^{-1} corresponded to the OH^- anions.

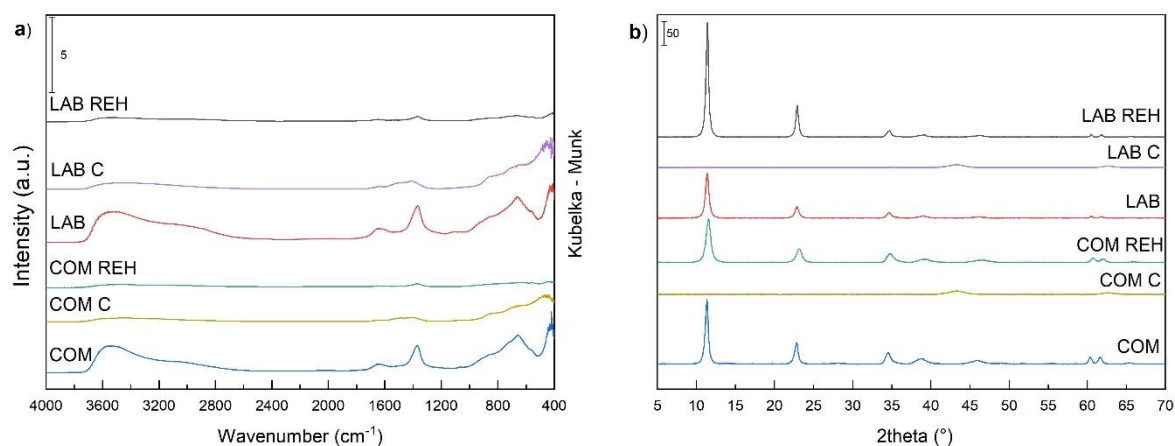


Figure 1. Diffuse reflectance infrared Fourier transform spectroscopy (DRIFT) (a) and X-ray diffraction (XRD) (b) and spectra of hydrotalcites (HTC) precursors, mixed oxides and rehydrated materials.

Calcination of samples at $450\text{ }^\circ\text{C}$ resulted in the disappearance of water, which is confirmed by the disappearance of the bands at around 1640 cm^{-1} and a shoulder around 3000 cm^{-1} (interlayer water molecules). As can be seen in Figure 1a, DRIFT spectra of calcined samples show the presence of residual carbonate anions and hydroxyl anions. A peak around 1400 cm^{-1} was observed because of the interaction between CO_3^{2-} and Mg^{2+} . There was a decrease in the intensity of bands around $3400\text{--}3500\text{ cm}^{-1}$, corresponding to the vibration of hydroxyl groups in layers, because of dihydroxylation [28–30]. M-OH and M-O-M (M is for metal) vibrations can be seen at bands at 470 , 680 and 790 cm^{-1} . Moreover, DRIFT spectra of samples after calcination show a minor presence of water, because of the air humidity during experiments, which is proved by a little peak around 1640 cm^{-1} and a broad band at around 3500 cm^{-1} , as well as residual carbonate anions from the air, adsorbed during the analysis.

X-ray diffractograms of the dried (HTC precursors) and rehydrated samples show the diffraction lines typical for the structure of hydrotalcite (Figure 1b). Typical reflections are at 11.3° , 22.8° , 34.6° , 39.1° , 46.2° , 60.3° and 61.8° . In the rehydrated sample of the commercial prepared hydrotalcite, a reflection shift from 11.3° to 11.5° was observed because of a degradation of the crystalline structure. Calcination at $450\text{ }^\circ\text{C}$ resulted in a destruction of the layered structure, as can be seen from the shape of the diffraction lines, which does not correspond to the typical structure of hydrotalcite. The structural changes caused by the calcination are characterized by two reflections at 43.3° and 62.7° that corresponds to MgO. The crystallite size and the interlayer distance (Table 1) in the dried samples was calculated using the first significant reflection (2theta of $\sim 11^\circ$). The crystallite size in the calcined samples was calculated using the reflection at 43.3° 2theta, corresponding to MgO.

Table 1. Structural properties of the studied samples after drying, calcination and rehydration.

Sample	LDH Crystallite Size D (nm)			LDH D Value (Å)		Relative Content of Crystalline Phases (%)	
	Dried	Rehydrated	Calcined	Dried	Rehyd	HTC	MgO
	HTC	HTC	HTC	Dried	Rehyd	HTC	MgO
COM	196.4	123.8	40.8	7.81	7.66	100	0
LAB	163.2	224.4	38.4	7.84	7.76	100	0

Rehydrated samples showed well-crystallized phases corresponding to the structure of reconstructed hydrotalcite. After the rehydration of samples, the interlayer distance decreased because of the replacement of the carbonate anions with hydroxyl anions. The difference in the interlayer distance was greater in the commercial hydrotalcite samples, where the interlayer distance decreased

after rehydration from 7.81 Å to 7.66 Å, while in the case of the laboratory prepared hydrotalcite samples, the interlayer distance only decreased from 7.84 Å to 7.76 Å. The dried commercial hydrotalcite samples had bigger crystallite size. After the rehydration of the samples, the crystallite size decreased in the commercial hydrotalcite samples from 196.4 Å to 123.8 Å, while it has been increased from 163.2 Å to 224.4 Å in the laboratory prepared samples. The commercial hydrotalcite samples showed a lower quality of the crystalline structure and overall smaller crystallite size after rehydration. This can be due to the addition of alumina during the extrusion process, because Al₂O₃ can disturb the rehydration process and it can also change the Mg/Al ratio in favour of Al. On the other hand, laboratory prepared hydrotalcite samples had much better crystalline structure because no additive was used during their synthesis, therefore the Mg/Al ratio closer to 3:1. Thus, it was possible to achieve 100% hydration and improvement of the crystalline structure. The crystallite size of the calcined samples was 38.4 Å and 40.8 Å for the laboratory prepared samples and commercial hydrotalcite samples.

Textural properties of the catalysts were determined by N₂-physisorption method. N₂-physisorption isotherms (Figure 2a) of dried and calcined laboratory prepared and commercial hydrotalcite samples show very different textural properties. As can be seen in Figure 3, the calcination step destroyed the HTC structure as confirmed by TGA-MS results and a large increase of mesopore volume and specific surface areas was observed (Table 2). Laboratory prepared samples possessed larger total pore volume than commercial samples. Calcination process resulted in the increase of total pore volume in both samples and in almost 100% increase in mesopore volume. Specific surface areas of laboratory prepared and commercial samples were very similar (around 75 m²/g). After the calcination, both samples showed an increase in specific surface area, up to three times of its original value. Specific surface area was greater in case of industrial samples, which might be due to the addition of alumina during the extrusion process of industrially prepared hydrotalcite. No micropores were observed in dried samples, both laboratory and commercial, and after calcination of these samples, there was only an insignificant volume of micropores. This can be due to the presence of water molecules and carbonate anions in the structure. After the calcination, the structure was released and individual layers drifted apart.

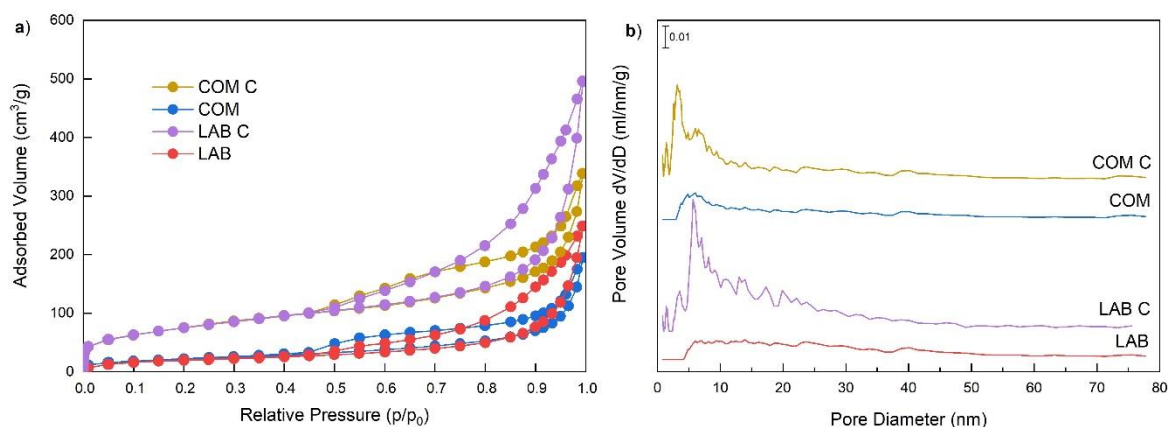


Figure 2. N₂ physisorption isotherms (a) and pore distribution (b) of HTC precursors and mixed oxides.

Table 2. Textural properties of HTC precursors and mixed oxides.

Sample	Specific Surface Area (m ² /g)	Total Pore Volume (cm ³ /g)	Micropore Volume (cm ³ /g)	Mesopore Volume (cm ³ /g)
COM	76.0	0.230	0.000	0.193
LAB	73.3	0.308	0.000	0.257
C COM	275.4	0.428	0.014	0.363
C LAB	241.9	0.654	0.007	0.588

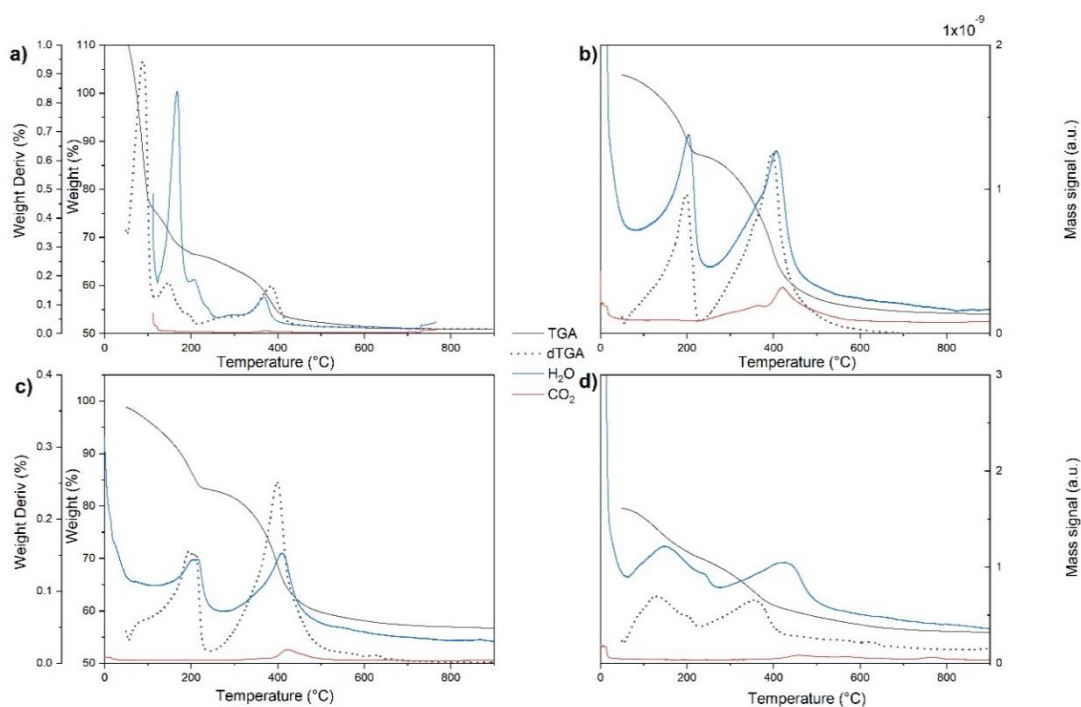


Figure 3. Thermogravimetric analysis with mass spectrometry detector (TGA-MS) analysis of laboratory prepared rehydrated material LAB REH (a), precursor LAB (b), commercially prepared precursor LAB (c) and rehydrated material COM REH (d).

As can be seen in Figure 2b, most of the pores in all samples had a diameter up to 50 nm. HTC precursors had a wide range of pores from 3 nm for industrial and 4 nm for laboratory synthesised. After calcination, the narrow dispersion of mesopores around 6 nm was observed for the LAB calcined sample and wider dispersion from 3 to 7 nm for C COM sample was observed.

TGA and DTG lines (Figure 3) show several phases of mass weight loss, because of thermal decomposition of samples. First, during the low-temperature mass loss, physically adsorbed water was removed, as can be seen especially in the R LAB sample. In the case of this sample, the first DTG peak was in a temperature range of 50 °C to around 100 °C, severe weight loss (over 37%) was evident because of the removal of residual water after rehydration and imperfect drying. The high-temperature mass loss started to occur at around 200 °C, where the physically adsorbed water was removed from all samples, as can be seen from corresponding signals on DTG lines. This was more evident in the case of dried samples. The next evident DTG peak was at around 400 °C and it was caused by the elimination of hydroxyl anions and carbonate anions from the interlayer space, as well as interlayer water. This DTG peak was also more severe in dried samples.

The individual charts (Figure 3) show the exact points of releasing water and CO₂. As can be seen, the peaks dedicated to water are evident and described above. As for the CO₂ in dried samples, the most CO₂ was released at approximately 400 °C. The peak was bigger and broader in the case of laboratory prepared dried sample. In both rehydrated samples, a little peak dedicated to CO₂ was also evident, because of the adsorption of CO₂ from the air during the measurement.

The total amount of the basic and acid sites was determined by TPD-NH₃ and TPD-CO₂ techniques. The obtained data are summarized in Table 3. A broad desorption peak of ammonia (Figure 4a) indicated large heterogeneity of the sample. The peaks at 103 °C and 101 °C in TPD-NH₃ for the laboratory prepared samples and commercial samples indicated the presence of weak acid sites. The shoulder of desorption peak in both samples is observed at 193 °C for LAB sample and 208 °C for COM sample. The shoulder showed the strong acid sites. The total amount of acid sites was higher in case of LAB samples in comparison with COM samples. However, the ratio of weak and strong acid

sites is the same for both COM and LAB samples. The acid sites can be attributed to the dehydration step of alcohols to condensates [31].

Table 3. Acid and base sites of the calcined samples determined by NH₃-TPD and CO₂-TPD experiments, respectively.

Sample	Gas	c _{SUM} (mmol/g)	T _{max1} (°C)	c _{LT} (mmol/g)	Population LT (%)	T _{max2} (°C)	c _{HT0} (mmol/g)	Population HT (%)
LAB	NH ₃	0.751	103	0.347	46	193	0.404	54
COM	NH ₃	0.555	101	0.255	46	208	0.300	54
LAB	CO ₂	1.192	112	0.699	59	194	0.494	41
COM	CO ₂	0.443	102	0.107	24	223	0.337	76

c_{SUM}—total concentration of acid sites (mmol/g); T_{max1}—the first temperature maximum (°C); c_{LT}—concentration of low-temperature acid sites (mmol/g); T_{max2}—the second temperature maximum (°C); c_{HT}—concentration of high-temperature acid sites (mmol/g).

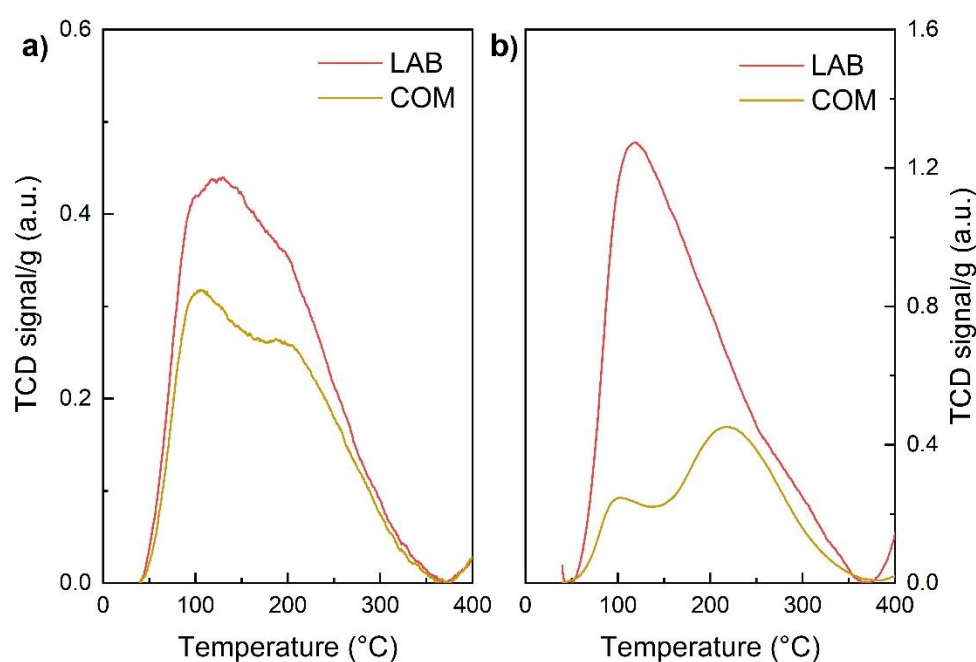


Figure 4. NH₃-TPD (a) and CO₂-TPD (b) of calcined samples.

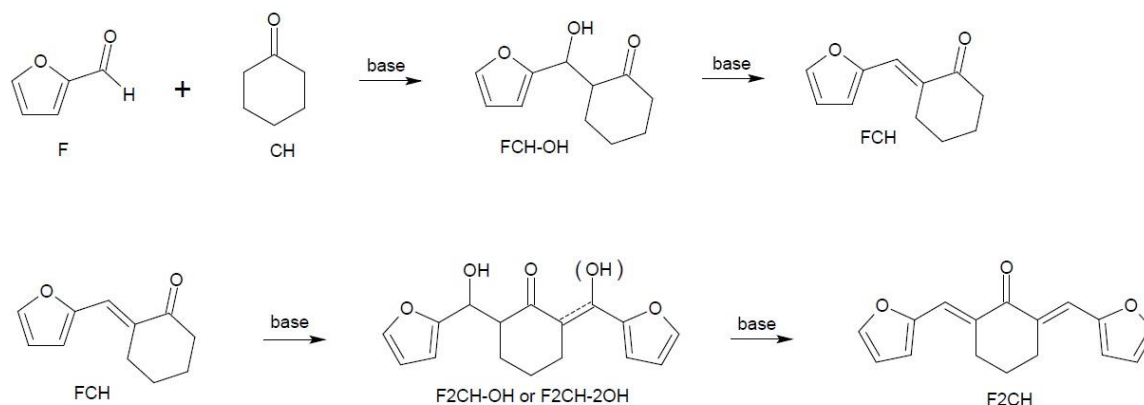
Broad desorption peaks of CO₂ are depicted in Figure 4b and showed a high distribution of basic sites. A desorption peak with a peak at 102 °C in COM samples and 112 °C in LAB samples corresponded to weak and moderate basic sites. Desorption peak at 223 °C in COM mixed oxide sample corresponded to strong basic sites. A shoulder was observed in LAB sample with desorption peak at around 194 °C which corresponded to the higher heterogeneity of the surface of LAB mixed oxide sample. The total amount of basic sites were three times higher in LAB sample in comparison with COM sample. A significantly higher amount of weak and moderate basic sites was observed in LAB sample. The active basic sites in aldol condensation are mainly Meⁿ⁺-O²⁻ pairs [31].

2.2. Catalytic Tests

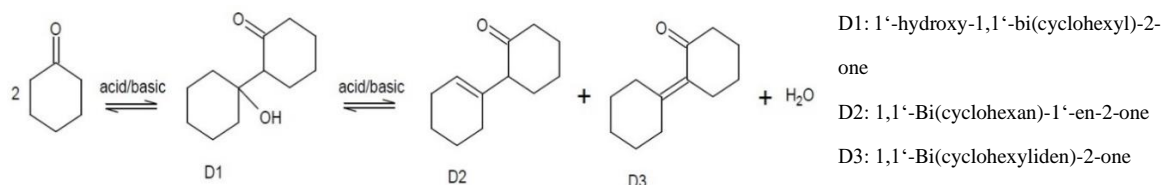
2.2.1. Aldol Condensation Mechanism

Aldol condensation of cyclohexanone (CH) and furfural (F) was carried out in a fixed-bed reactor described earlier in the article. The catalyst samples denoted as COM and LAB were tested. The reaction has gone through several consequent phases, wherein the primary step was a reaction between CH and F (depicted in Scheme 1). First product is FCH-OH (2-[2-furyl(hydroxyl)methyl]-cyclohexanone),

which is an alcoholic intermediate, that subsequently undergoes dehydration, which results in creating the second product of the condensation, FCH ((2E)-2-[2-furyl-methylene]-cyclohexanone). FCH can react with another furfural molecule to create the next product, F2CH ((2E,6E)-2,6-bis [2-furyl-methylene]-cyclohexanone), before that, its precursors are created, F2CH-OH and F2CH-2OH, which undergo dehydration. A major side reaction may occur, in which the cyclohexanone undergoes self-condensation, resulting in the formation of the CHCH (1'-hydroxy-1,1'-bi(cyclohexyl)-2-one) from two CH molecules. The self-condensation of cyclohexanone (depicted in Scheme 2) may cause a decrease in the CH concentration in the reaction mixture.



Scheme 1. Aldol condensation of furfural and cyclohexanone.



Scheme 2. Self-condensation of cyclohexanone.

2.2.2. Test No. 1—Rehydrated and Regenerated LAB Catalyst

In LAB catalysts, the highest catalytic activity was observed in test No. 1 (rehydrated catalyst) (Figure 5). The rehydrated laboratory prepared catalyst exhibited very high activity (100% conversion of F) for 55 h on stream (Figure 5a) which then started to decline. The activity of the catalyst was very high from the beginning of the test.

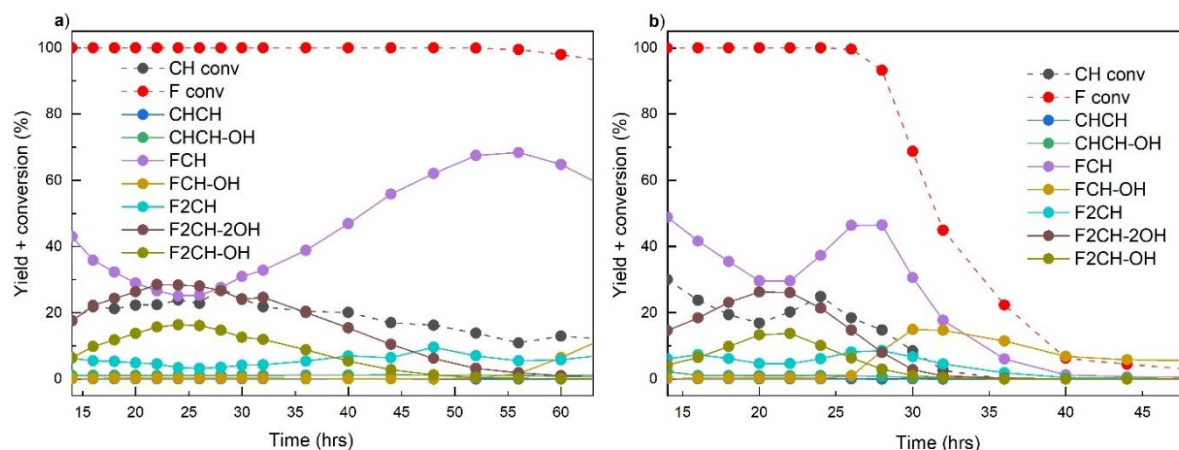


Figure 5. Catalytic test with LAB catalyst—test No. 1 (rehydrated (a) and regenerated (b) catalyst).

The initial yield of FCH was high (43 wt.%). Then, the FCH product reacted with another molecule of F to F2CH-OH and F2CH-2OH alcohols resulting in maximum production of ca. 29 wt.% for F2CH-2OH and 16 wt.% for F2CH-OH after 25 h on stream.

The dehydrated final product F2CH was observed in the reaction mixture in the low content (up to 9 wt.%) this suggested that dehydration of the corresponding alcohols was not as easy as dehydration of FCH-OH and was much slower. After 25 h on stream, the F2CH-OH and F2CH-2OH yields were gradually decreased while the FCH yield was steadily increased. That later culminated at 55 h on stream where the catalyst slowly deactivated. At the same time period the yield of F2CH remained almost constant. FCH-OH spontaneously split the water off, and its content was higher when the deactivation of the catalyst started. The test was stopped after 64 h and the catalyst was subsequently regenerated by calcination in the air and again rehydrated before the catalytic test. The obtained results (Figure 5b) show that regeneration of catalyst followed by rehydration led to a lower catalytic performance because of the structural changes in the catalyst. The 100% conversion of furfural was observed for up to 26 h of the test followed by a very rapid decline (Figure 5b).

The product composition was very similar to the previous test with the fresh catalyst. At first, when the catalytic activity was high, a great share of alcohols F2CH-OH (up to 14%) and F2CH-2OH (up to 27%) was observed. The F2CH condensate content was relatively low (up to 10%), thus, it can be seen that dehydration of these alcohols was more complicated than dehydration of the FCH-OH, which was also observed in the mixture, but again, not until the beginning of the catalyst deactivation and the decrease of furfural conversion less than 100%. The test was finished after almost complete catalyst deactivation (when the furfural conversion was just a few %). Yields of cyclohexanone self-condensation products (CH-CH and CHCH-OH) are negligible, typically up to 0.3% and 1.2%, respectively.

The analysis of the used catalyst showed that the catalyst contained hydrotalcite phase only (Figure S1), but with lower crystallinity (Table S1), than the original rehydrated catalyst. The interlayer distance was also different (Table S1) and it suggests that one of the possible causes of deactivation was a transformation of the catalyst from the hydroxyl form (only OH groups in the interlayer space) to the carbonate form (where the interlayer space contains $(\text{CO}_3)_2$ anion).

CO_2 and H_2O co-products were formed during the reactions in the fixed-bed reactor. CO_2 forms because of the 2-furoic acid decomposition, which is created by the Cannizzaro reaction from furfural [19]. H_2O was formed during the dehydration of aldol products, mainly FCH-OH. Another cause of catalytic deactivation was the formation of carbon deposits, which may directly deactivate catalytic centres and also take a place in the interlayer space in the form of organic acid anions instead of OH groups in the rehydrated catalyst. But, considering the LDH D value 7.85 Å this version is unlikely, because organic anions are causing that the layers drift apart more. For example, LDH D value for acetate anion is around 11 Å, for benzoic acid anion over 12 Å, etc. [23]. The used catalyst contained a significant amount of carbon (14.9 wt.%), although the part made out of carbonate anions in interlayer space of HTC precursor was only around 2% and the rest were carbon deposits.

Textural properties of the used catalyst were very similar to the laboratory prepared HTC precursor. In almost all aspect, including specific surface, total volume, mesopore volume and TGA results of the used catalyst, that were made in N_2 atmosphere, the decomposition process was the same as in the case of HTC precursors. Considering the carbon deposits and subsequent regeneration of the catalyst (in situ calcination) in the reactor, the measuring was done in the O_2 atmosphere with the same parameters and then with isotherm 180 min at temperature 450 °C (Figure 6). These set conditions were simulating the regeneration process of the catalyst. A great decrease in weight was observed from the temperature of 250 °C caused by the beginning of the carbon deposits decomposition. In the TGA-MS record, a higher share of H_2O and CO_2 was detected. Isothermal measurement at 450 °C showed the removal of practically all deposits in the first 60 min. Long-term weight loss (120 min) was very small, changes were in the order of tenths of wt.%.

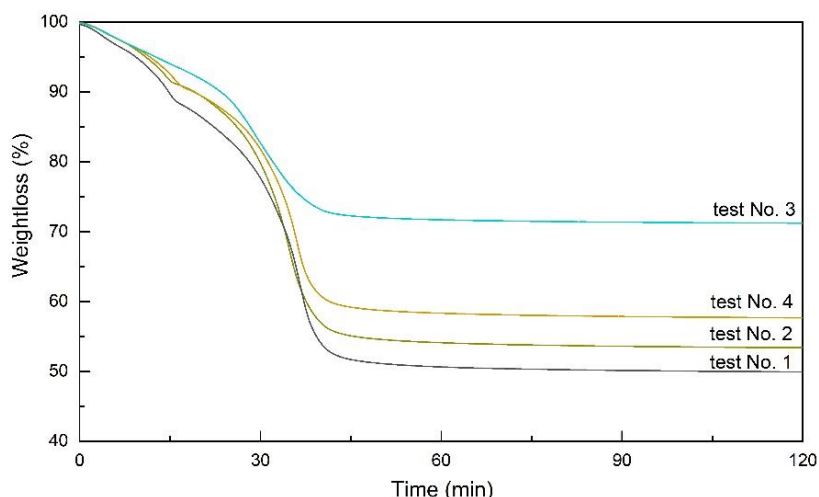


Figure 6. Thermogravimetric analysis (TGA) of used catalysts (O_2 , isotherm $450^\circ C$).

DRIFT spectra of all the used catalyst samples (Figure S1b) showed much more bands, thus according to the DRIFT spectra database, these bands found to be ascribed to the organic deposits on the catalyst and the corresponding bonds have been identified ($C=O$, $C=C$, CH , CH_2 , CH_3 , $-C-O-C-$).

Lower catalytic activity after regeneration and rehydration was also probably because of the disruption of the active sites because of leaching of the components into the product mixture. The higher Mg content of the reaction products was usually observed at the beginning of the tests for the rehydrated catalysts Test 1 and Test 3 (Figure 7a,d) and gradually stabilized during the test. Al was released from the catalysts only in a very small amount. The presence of Fe in the product mixture was observed due to reactor corrosion. The initial presence of Fe was caused by surface oxidation of the steel reactor before the catalyst loading, after its regeneration or rehydration, and was evident in all Tests 1 to 4 (Figure 7a–e). After stabilization of the Fe content during aldol condensation, there was a significant increase after 26 h (Figure 7b). This interval corresponded to the time of decline in catalytic activity and may have been associated with increased acidity of the reaction products.

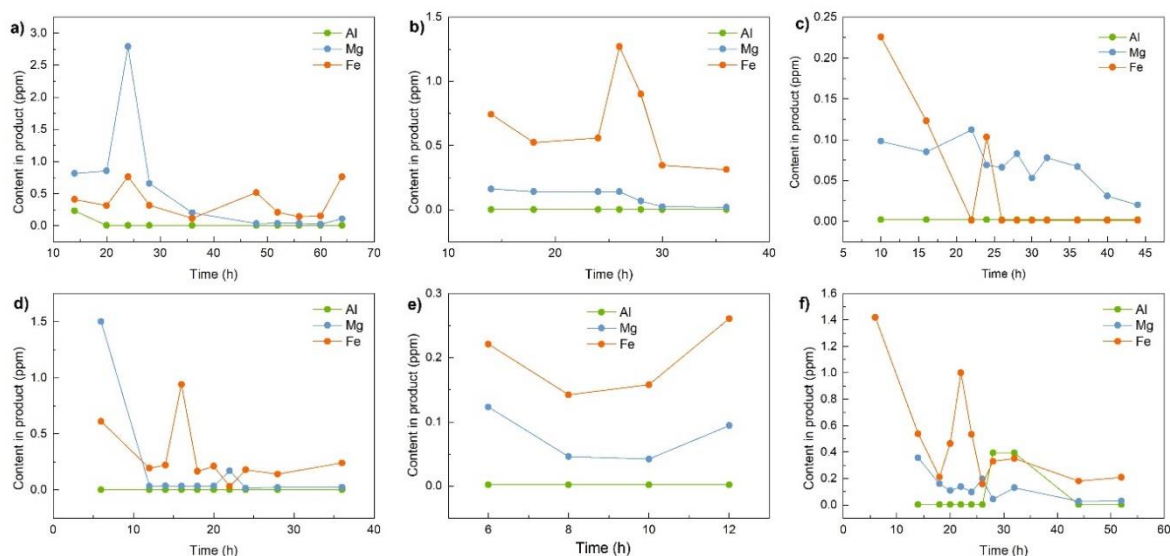


Figure 7. Metal content in aldol product (test No. 1 (a), test No. 1 regenerated (b), test No. 2 (c), test No. 3 (d), test No. 3 regenerated (e), test No. 4 (f)).

2.2.3. Test No. 2—Calcined LAB Catalyst

During the test No. 2, where calcined catalyst without rehydration was used, much shorter time of 100% furfural conversion (24 h) and gradual catalyst deactivation was observed (Figure 8). After 54 h, the furfural conversion was still 50%. Product composition was different compared to the previous test. F2CH-OH alcohols content decreased from the beginning of the test along with gradual deactivation of the most active sites of the catalyst (primary content of both was about 20%). Dehydrated F2CH product content was up to 9% again. At 24 h, FCH condensate content in the reaction mixture was almost 60%, and the FCH-OH product content gradually started to increase.

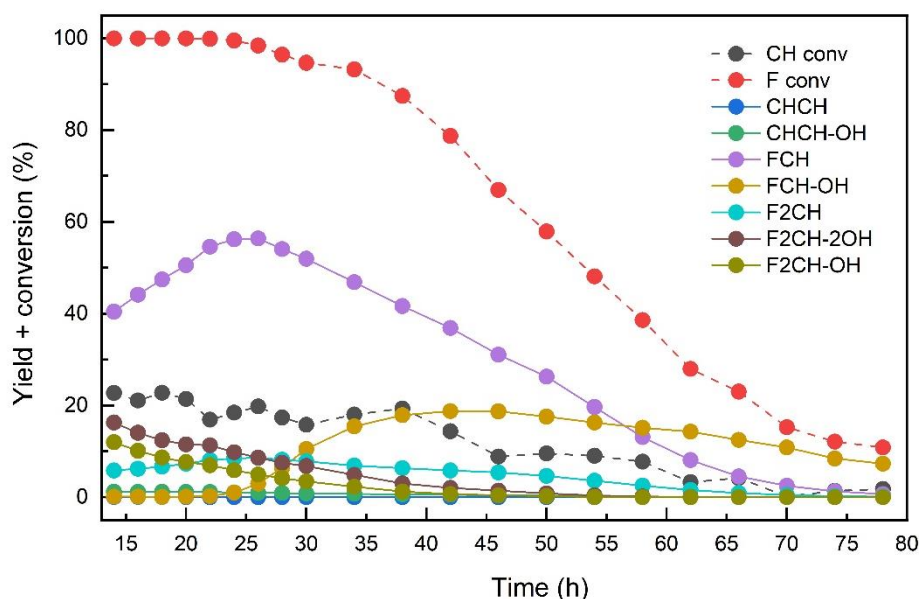


Figure 8. Catalytic test with LAB catalyst—test No. 2 (calcined catalyst).

The used catalyst was, as before, fully rehydrated and converted to the carbonate form (Figure S1a, Table S1). Carbon content was similar (14.5 wt.%), with the same distribution of carbon components (DRIFT data Figure S1b). Because the calcined form of the catalyst was used, there is soft, gradual rehydration during the test and differences in texture are obvious (Figure S2). The catalyst possessed not only lower specific surface area but also a significantly lower amount of mesopores (Table S2). Leaching of metals is very low, mainly the increase of Mg in the product mixture is observed (Figure 7c).

2.2.4. Test No. 3—Calcined and Regenerated COM Catalyst

In commercial catalyst (COM samples), the catalytic activity was generally much lower in comparison with LAB samples, but the product composition was very similar.

The commercial catalyst performed 100% conversion for up to 18 h (Figure 9a). After that, it started to decrease and from this moment, the concentration of the final product F2CH (up to 9%, as in the test No. 1) started to decrease along with the FCH concentration (that was up to 50%). At the beginning of the test, F2CH-OH product slightly increased to over 20% and then gradually decreased until the end of the test (after 44 h) when the furfural conversion was at 20%. The catalyst was subsequently regenerated at the same conditions as in the test No. 1 (without rehydration of catalyst) and tested again (Figure 9b). In comparison with the test No. 2 (where only calcined catalyst without subsequent rehydration was used) it is obvious that both types of catalysts (COM and LAB) showed similar product composition, but in the case of the commercial catalyst sample, there is faster deactivation and time of 100% furfural conversion is up to 30% shorter.

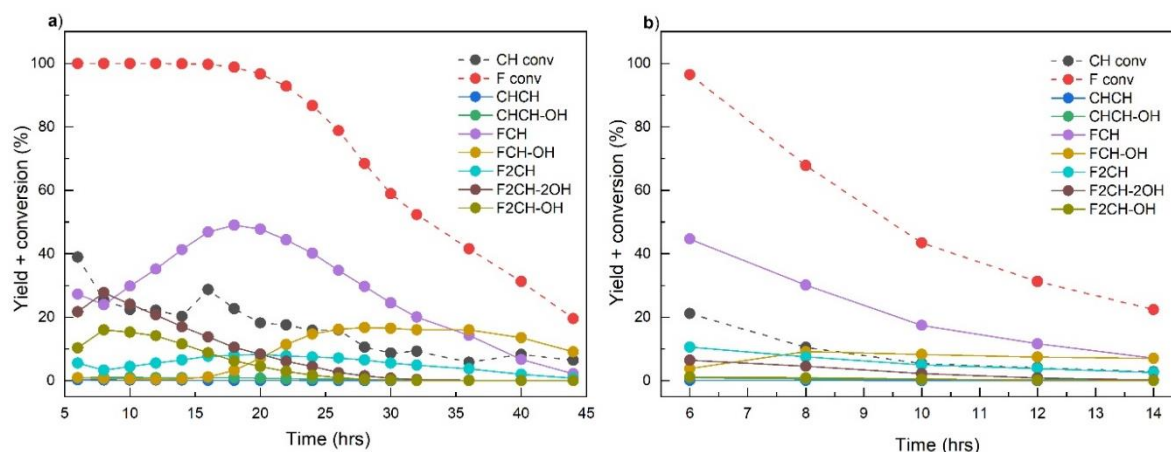


Figure 9. Catalytic test with COM catalyst—test No. 3 (rehydrated (a) and regenerated (b) catalyst).

The initial activity of the regenerated catalyst was below 100% of furfural conversion and started to decrease immediately after starting the test. It is because the catalyst was damaged during the process (decrease in Mg etc.) and the regeneration was not successful. Almost all product also decreased from the beginning, except FCH-OH which was increasing for 8 h and then decreased. The test was ended after 14 h when the conversion of furfural was only about 20%.

XRD analysis of used catalysts showed that the sample contained both hydrotalcite and MgO phase (Figure S1). It also had a different colour (light brown) than the rest of the samples which were dark brown, almost black. The carbon content was lower only 9.55%. The reason for this was that there was a low activity after regeneration of the catalyst and the rehydration process was unsuccessful. Thus, the sample contained HTC crystal phase (29.4%) as well as MgO crystal phase (70.6%) which is summarized in Table S1. Also, the interlayer distance in this sample was slightly lower than in other samples. In comparison with the fresh catalyst samples, the used catalyst samples possessed higher D value and much lower crystallite size.

Textural properties of used catalysts also showed significant differences. N₂-physisorption isotherms and pore distributions (Figure S2) showed other pores for used catalysts. As can be seen, there were no micropores in any of the used catalysts and higher amount of macropores was observed (Table S2). Overall the used catalyst samples had a lower specific surface area. There has been a decrease in the total pore volume and mesopore volume. The higher surface area of used (regenerated) catalyst (than hydrotalcite precursor) also showed imperfect rehydration and it was due to a higher mixed oxide content, which had a high specific surface area (over 270 m²/g). Again, these changes were attributed to the structural changes in the catalyst during the regeneration.

2.2.5. Test No. 4—Calcined COM Catalyst with High Purity Cyclohexanone

The highest catalytic activity was observed in the 4th test using a cleaner, higher-quality feedstock (purity of CH higher than 99.9%). There was 100% furfural conversion for almost 25 h and after that, it gradually decreased (Figure 10). FCH content increased until 25 h, then decreased along with the furfural conversion. At this point, the FCH-OH concentration started to increase. At the time of 40 h, the furfural conversion was at 60%, which was much higher in comparison with previous test. The concentration of the final product F2CH (almost 12%) was also greater. The test was ended after 56 h when the catalytic activity was low and the furfural conversion was still over 22%.

The results show that the purity of the feedstock has a significant influence on the catalyst deactivation, which is probably caused by impurities contained in feedstocks.

Unlike the previous test, the catalyst regeneration was not done because of obtaining important information about the catalyst after the reaction.

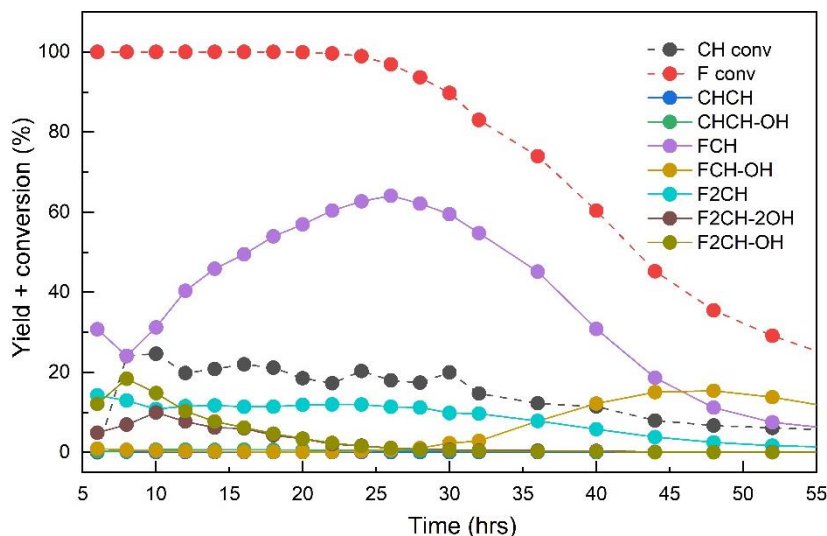


Figure 10. Catalytic test with COM catalyst—test No. 4.

From the data obtained, in particular, from the X-ray diffraction (Figure S1, Table S1), it can be seen that the catalyst contained only the hydrotalcite phase after the reaction, with parameters (interlayer distance, crystallite size) similar to the hydrotalcite precursor. There was only a slight decrease in the specific surface area and the pore volume (Figure S2, Table S2). It suggests that the cause of the structural defects in the catalyst, that makes subsequent regeneration/rehydration impossible, is probably the thermal stress during the attempt to regenerate the catalyst, not the process of the aldol condensation.

TGA results (Figure 6) made in the O₂ atmosphere (with the same parameters as previous tests) showed a great decrease in weight because of the carbon deposits decomposition (carbon content 11.4%) after reaching 250 °C and removing all the deposits within the first 60 min during the isothermal measurement at 450 °C (as well as in the case of the test No. 1).

As in the previous test, there was a presence of Fe in the product mixture from the beginning caused by reactor corrosion and increasing of its content during the experiment indicated the formation of highly reactive products. Also, there was a higher amount of Al after 26 h, than in previous tests (Figure 7f).

3. Materials and Methods

3.1. Synthesis of Catalyst

Mg–Al hydrotalcite precursor (Mg:Al molar ratio 3:1) was synthesized by the same method of synthesis as in reference [22] (co-precipitation at constant pH value (pH = 9.5) and constant temperature (T = 60 °C)). Mixed aqueous solution of magnesium nitrate Mg(NO₃)₂·6H₂O (Lachner, p.a. purity) and aluminium nitrate Al(NO₃)₃·9H₂O (Lachner, p.a. purity) (c_{Mg+Al} = 1 mol/dm³) was precipitated with basic solution containing potassium carbonate K₂CO₃ (Penta, p.a. purity) and potassium hydroxide KOH (Lachner, p.a. purity) (c_{KOH} = 2 mol/dm³ + c_{K₂CO₃} = 0.2 mol/dm³). The solid was separated by press-filtration using paper filter plate; the filter cake was washed with demineralised water until neutral pH was achieved and dried in an oven overnight at 65 °C. Samples were denoted as LAB.

Commercial HTC with Mg/Al molar ratio 3:1 provided by Eurosupport Manufacturing Czechia (ESMC) was denoted COM. The calcined versions of samples were denoted with “C” in front of the name of the sample, rehydrated, regenerated with “R” and used catalyst were denoted with “U”.

3.2. Catalytic Tests

The experiments were carried out in a stainless steel fixed-bed reactor, 700 mm long with an inner diameter of 17 mm. The reactor was equipped with 5-mm wide thermo tube and three thermocouples located at the beginning, the centre and the end of the catalytic bed. The experimental unit was located in UniCRE (Unipetrol Centre of Research and Education) in Litvínov, Czech Republic. Prior to the experiment, the reactor was loaded with the catalyst (fraction 224–560 μm , 5 g) and SiC (0.1 mm) mixture (1:1). Above and below the layer of the catalyst, layers of SiC (1–2 mm) were placed. All individual layers were separated by quartz wool plugs.

First, catalysts were calcined in situ at 450 °C for 4 h (N_2 , 5 l/h, temperature ramp 100 °C/h). After the activation, the temperature was decreased to 80 °C, the pressure was set at 1 MPa and the nitrogen flow was set to 5 l/h.

In the test with the catalyst rehydration, distilled water was pumped into the reactor (10 g/h for 8 h) to rehydrate the catalyst.

Then the feedstock (a mixture of cyclohexanone and furfural (5:1) 10 g/h, both +99% purity) was pumped into the reactor (WHSV 2 h^{-1}) and product mixtures were analysed by an Agilent 7890A (Agilent Technologies Inc., Santa Clara, CA, USA) gas chromatograph equipped with a flame ionization detector (FID), using a HP 5 capillary column (30 m/0.32 mm ID/0.25 μm).

After the last sample was taken, the catalyst was regenerated: the unit was flushed with methanol for 10 h and subsequently with nitrogen for 6 h. Then the air flow was set for 40 l/h and the temperature was set first at 250 °C (1 h), 350 °C (1 h) and finally at 450 °C (4 h). In general, the experiments showed a good agreement with the results. Because of high time-consumption and economical demands, it was not possible to reproduce all the experiments.

Test parameters are listed in the Table 4.

Table 4. Parameters of catalytic tests.

No. of Test	Catalyst	Regeneration	Rehydration
1.	LAB	YES	YES
2.	LAB	NO	NO
3.	COM	YES	NO
4.	COM	NO	NO

3.3. Characterisation of Precursors and Catalysts

To verify the chemical composition, an ICP-EOS Agilent 725 (Agilent Technologies Inc., Santa Clara, CA, USA) was used. Prior to the analysis, 500 mg of sample was dissolved in 10 mL of H_2SO_4 (1:1) and heated. Afterward, the mixture was cooled down, diluted with demineralized water and heated to 100 °C for a couple of minutes. Then the mixture was poured into a volumetric flask and analysed.

The crystallographic structure of the samples was determined using the X-ray diffraction (XRD) patterns. Powdered samples were obtained using the D8 Advance ECO (Bruker AXS GmbH, Karlsruhe, Germany.) with $\text{CuK}\alpha$ radiation ($\lambda = 1.5406 \text{ \AA}$). The step size of 0.02° and a step time of 0.5 s were used. The XRD patterns were collected in the range from 5° to 70° 2theta and evaluated using the Diffrac.Eva software (Bruker AXS GmbH, Karlsruhe, Germany) and the Powder Diffraction File database (PDF 4+ 2018, International Centre for Diffraction Data, Newtown Square, PA, USA).

Diffuse reflectance infrared Fourier transform spectroscopy (DRIFT) spectra were obtained using the Nicolet iS 10–Thermo Scientific (Waltham, MA, USA). First, 15 mg of the sample was mixed with 300 mg KBr and analysed. The parameters of the analysis were the following: number of scans 128, resolution 2 cm^{-1} .

Specific surface area (BET), pore distribution and pore volume were determined by N_2 -adsorption/desorption at -196 °C using an Autosorb iQ (Quantachrome Instruments Boynton

Beach, FL, USA). Prior the analysis, all samples were dried under vacuum for 16 h at 110 °C in a glass-cell.

Thermogravimetric analysis (TGA) was obtained using the TA Instruments TGA Discovery series (TA Instruments, Lukens Drive, NW, USA) operating at a heating ramp 10 °C/min in a temperature range from 40 to 900 °C in the flow of nitrogen (20 mL/min, Linde 5.0). Approximately 15 mg of sample was put inside an open alumina crucible and heated. To detect the fragments, the Quadrupole mass detector OmniStar GSD320 (Pfeiffer Vacuum Austria GmbH, Vienna, Austria) was used. SCAN mode with voltage 1450 V of electron multiplier were used for measuring.

Acid-base properties of the materials were determined with CO₂ and NH₃ temperature-programmed desorption (TPD) using the Autochem 2950 HP (Micromeritics Instrument Corporation, Norcross, GA, USA). Typically, the amount of 100 mg of sample was put into a quartz U-tube reactor, which was pretreated in He to 500 °C with a heating rate of 10 °C/min. In the case of NH₃-TPD, the sample was cooled down to 50 °C and then it was saturated with ammonia for 30 min (25 mL/min of 10 vol.% NH₃/He). Then the gas was switched to helium (25 mL/min) in order to remove weakly adsorbed ammonia molecules and the flushing continued until the baseline was constant (60 min). After the procedure, the temperature was set to 900 °C with a heating rate of 15 °C/min in order to obtain the NH₃-TPD curves. The CO₂-TPD sample was pretreated the same way as the NH₃-TPD sample. Subsequently, the sample was cooled down to 50 °C and the gas was switched to the mixture of 10 vol.% CO₂/He (25 mL/min). Then the sample was saturated with CO₂ for 30 min. Then, the gas was switched to helium for one hour at 50 °C in order to remove weakly adsorbed molecules. To obtain the TPD curves, the temperature was increased from 50 °C to 900 °C with a heating rate of 15 °C/min. The changes in the gas concentration were monitored using a TCD detector.

4. Conclusions

Catalytic activity of commercial and laboratory synthesized Mg/Al mixed oxides was compared in aldol condensation of cyclohexanone and furfural. Catalysts based on rehydrated mixed oxides were prepared by calcination of the hydrotalcite precursors and their subsequent in situ rehydration inside the reactor. During the tests, a very good catalytic activity was observed. During the set conditions (80 °C, CH:F = 5:1, 10 g/h) and using laboratory prepared catalyst, 100% furfural conversion was observed for more than 55 h. The yield of condensation products FCH and F2CH was up to 68% and 10%, respectively. In the beginning, a relatively large share of non-dehydrated condensation products (F2CH-OH and F2CH-2OH, up to 16% and 28% respectively) was observed in the reaction mixture. This fact means that unlike the condensation product, which undergoes dehydration fast (FCH-OH to the final product FCH), the dehydration of the above-mentioned products was much slower. The deactivated catalyst was then regenerated in situ by calcination and rehydration; however, subsequent results pointed out structural changes in the catalyst that caused the catalyst deactivation much faster (100% furfural conversion only for the time of 26 h). On the other hand, in the case of commercial catalyst, the results were not so good (100% furfural conversion up to 18 h), but the product composition was similar to the previous test. During the test (meaning the regeneration of commercial catalyst) there were significant structural changes, which made it impossible to achieve full regeneration. The catalyst was not able to reach a 100% furfural conversion and its activity was falling fast. That may be due to the addition of Al₂O₃ during the extrusion step of the synthesis. The purity of feedstock had a significant influence on the catalytic activity. Using the cyclohexanone of >99.9% purity extended the time of 100% furfural conversion by 1/3. The obtained data showed, that the Mg/Al mixed oxides based heterogeneous catalysts are suitable for using in the aldol condensation of furfural and cyclohexanone, which is one of the alternative ways to obtain fuels from renewable sources.

Supplementary Materials: The following are available online at <http://www.mdpi.com/2073-4344/9/12/1068/s1>, Figure S1: XRD and DRIFT spectra of used catalysts, Figure S2: N₂ physisorption isotherms (a) and pore distribution (b) of used catalysts, Table S1: Diffraction and phase properties of the used catalysts, Table S2: Textural properties of used catalysts.

Author Contributions: Conceptualization, Z.T.; data curation, Z.T.; investigation, P.V.; resources, K.H., J.K., K.Š. and R.V.; supervision, Z.T., visualisation, E.S.; writing—original draft, Z.T. and E.S.; writing—review and editing, Z.T., J.K. and K.H.

Funding: The publication is a result of the project Development of the UniCRE Centre (LO1606) which has been financially supported by the Ministry of Education, Youth and Sports of the Czech Republic (MEYS) under the National Sustainability Programme I. The result was achieved using the infrastructure of the project Efficient Use of Energy Resources Using Catalytic Processes (LM2015039) which has been financially supported by MEYS within the targeted support of large infrastructures.

Conflicts of Interest: The authors declare no conflict of interest. The funders had no role in the design of the study; in the collection, analyses, or interpretation of data; in the writing of the manuscript, or in the decision to publish the results.

References

1. Huber, G.W.; Iborra, S.; Corma, A. Synthesis of Transportation Fuels from Biomass: Chemistry, Catalysts, and Engineering. *Chem. Rev.* **2006**, *106*, 4044–4098. [[CrossRef](#)] [[PubMed](#)]
2. Huber, G.W.; Dale, B.E. Grassoline at the Pump. *Sci. Am.* **2009**, *301*, 52–59. [[CrossRef](#)] [[PubMed](#)]
3. Kubička, D.; Kubičková, I.; Čejka, J. Application of Molecular Sieves in Transformations of Biomass and Biomass-Derived Feedstocks. *Catal. Rev.* **2013**, *55*, 1–78. [[CrossRef](#)]
4. Somerville, C.; Youngs, H.; Taylor, C.; Davis, S.C.; Long, S.P. Feedstocks for Lignocellulosic Biofuels. *Science* **2010**, *329*, 790–792. [[CrossRef](#)]
5. Zinoviev, S.; Müller-Langer, F.; Das, P.; Bertero, N.; Fornasiero, P.; Kaltschmitt, M.; Centi, G.; Miertus, S. Next-Generation Biofuels: Survey of Emerging Technologies and Sustainability Issues. *ChemSusChem* **2010**, *3*, 1106–1133. [[CrossRef](#)]
6. Barrett, C.; Chheda, J.; Huber, G.; Dumesic, J. Single-Reactor Process for Sequential Aldol-Condensation and Hydrogenation of Biomass-Derived Compounds in Water. *Appl. Catal. B Environ.* **2006**, *66*, 111–118. [[CrossRef](#)]
7. Kikhtyanin, O.; Hora, L.; Kubička, D. Unprecedented Selectivities in Aldol Condensation over Mg–Al Hydrotalcite in a Fixed Bed Reactor Setup. *Catal. Commun.* **2015**, *58*, 89–92. [[CrossRef](#)]
8. Hu, X.; Wu, L.; Wang, Y.; Song, Y.; Mourant, D.; Gunawan, R.; Gholizadeh, M.; Li, C.-Z. Acid-Catalyzed Conversion of Mono- and Poly-Sugars into Platform Chemicals: Effects of Molecular Structure of Sugar Substrate. *Bioresour. Technol.* **2013**, *133*, 469–474. [[CrossRef](#)]
9. Chheda, J.N.; Huber, G.W.; Dumesic, J.A. Liquid-Phase Catalytic Processing of Biomass-Derived Oxygenated Hydrocarbons to Fuels and Chemicals. *ChemInform* **2007**, *38*. [[CrossRef](#)]
10. Dodds, D.R.; Gross, R.A. Chemicals from Biomass. *Science* **2007**, *318*, 1250–1251. [[CrossRef](#)]
11. Silva, C.C.C.; Ribeiro, N.F.; Souza, M.M.; Aranda, D.A. Biodiesel Production from Soybean Oil and Methanol Using Hydrotalcites as Catalyst. *Fuel Process. Technol.* **2010**, *91*, 205–210. [[CrossRef](#)]
12. Endalew, A.K.; Kiros, Y.; Zanzi, R. Inorganic Heterogeneous Catalysts for Biodiesel Production from Vegetable Oils. *Biomass Bioenergy* **2011**, *35*, 3787–3809. [[CrossRef](#)]
13. Semwal, S.; Arora, A.K.; Badoni, R.P.; Tuli, D.K. Biodiesel Production Using Heterogeneous Catalysts. *Bioresour. Technol.* **2011**, *102*, 2151–2161. [[CrossRef](#)] [[PubMed](#)]
14. Hora, L.; Kikhtyanin, O.; Čapek, L.; Bortnovskiy, O.; Kubička, D. Comparative Study of Physico-Chemical Properties of Laboratory and Industrially Prepared Layered Double Hydroxides and Their Behavior in Aldol Condensation of Furfural and Acetone. *Catal. Today* **2015**, *241*, 221–230. [[CrossRef](#)]
15. Kikhtyanin, O.; Tišler, Z.; Velvarská, R.; Kubička, D. Reconstructed Mg–Al Hydrotalcites Prepared by Using Different Rehydration and Drying Time: Physico-Chemical Properties and Catalytic Performance in Aldol Condensation. *Appl. Catal. A General* **2017**, *536*, 85–96. [[CrossRef](#)]
16. Tichit, D.; Bennani, M.N.; Figueras, F.; Tessier, R.; Kervennal, J. Aldol Condensation of Acetone over Layered Double Hydroxides of the Meixnerite Type. *Appl. Clay Sci.* **1998**, *13*, 401–415. [[CrossRef](#)]
17. Figueras, F. Base Catalysis in the Synthesis of Fine Chemicals. *Top. Catal.* **2004**, *29*, 189–196. [[CrossRef](#)]
18. Faba, L.; Díaz, E.; Ordóñez, S. Aqueous-Phase Furfural-Acetone Aldol Condensation over Basic Mixed Oxides. *Appl. Catal. B Environ.* **2012**, *113–114*, 201–211. [[CrossRef](#)]

19. Vrbková, E.; Tišler, Z.; Vyskočilová, E.; Kadlec, D.; Červený, L. Aldol Condensation of Benzaldehyde and Heptanal: A Comparative Study of Laboratory and Industrially Prepared Mg–Al Mixed Oxides. *J. Chem. Technol. Biotechnol.* **2017**, *93*, 166–173. [[CrossRef](#)]
20. Kuśtrowski, P.; Sułkowska, D.; Chmielarz, L.; Rafalska-Łasocha, A.; Dudek, B.; Dziembaj, R. Influence of Thermal Treatment Conditions on the Activity of Hydrotalcite-Derived Mg–Al Oxides in the Aldol Condensation of Acetone. *Microporous Mesoporous Mater.* **2005**, *78*, 11–22. [[CrossRef](#)]
21. Kikhtyanin, O.; Lesnik, E.; Kubička, D. The Occurrence of Cannizzaro Reaction over Mg–Al Hydrotalcites. *Appl. Catal. A General* **2016**, *525*, 215–225. [[CrossRef](#)]
22. Cavani, F.; Trifirò, F.; Vaccari, A. Hydrotalcite-Type Anionic Clays: Preparation, Properties and Applications. *Catal. Today* **1991**, *11*, 173–301. [[CrossRef](#)]
23. Diko, M. Fourier Transform Infrared Spectroscopy and Thermal Analyses of Kaolinitic Clays from South Africa and Cameroon. *Acta Geodyn. Geomat.* **2015**, 149–158. [[CrossRef](#)]
24. Wahab, R.; Ansari, S.G.; Kim, Y.S.; Dar, M.A.; Shin, H.-S. ChemInform Abstract: Synthesis and Characterization of Hydrozincite and Its Conversion into Zinc Oxide Nanoparticles. *ChemInform* **2008**, *39*. [[CrossRef](#)]
25. Jiang, W.; Lu, H.-F.; Qi, T.; Yan, S.-L.; Liang, B. Preparation, Application, and Optimization of Zn/Al Complex Oxides for Biodiesel Production under Sub-Critical Conditions. *Biotechnol. Adv.* **2010**, *28*, 620–627. [[CrossRef](#)] [[PubMed](#)]
26. Li, J.; Yu, Y.; Zhang, L. Bismuth Oxyhalide Nanomaterials: Layered Structures Meet Photocatalysis. *Nanoscale* **2014**, *6*, 8473–8488. [[CrossRef](#)]
27. Roy, D.M.; Roy, R.; Osborn, E.F. The System MgO–Al₂O₃–H₂O and Influence of Carbonate and Nitrate Ions on the Phase Equilibria. *Am. J. Sci.* **1953**, *251*, 337–361. [[CrossRef](#)]
28. Allegra, G.; Ronca, G. Crystal Powder Statistics. II. Line Profiles in Diffraction Spectra of Identical Crystals and of Gaussian Samples. Crystal Size Distributions. *Acta Crystallogr. Sect. A* **1978**, *34*, 1006–1013. [[CrossRef](#)]
29. López-Salinas, E.; García-Sánchez, M.; Ramon-Garcia, M.L.; Schifter, I. New Gallium-Substituted Hydrotalcites: [Mg_{1-x}Ga_x(OH)₂](CO₃)_{x/2}·mH₂O. *J. Porous Mater.* **1996**, *3*, 169–174. [[CrossRef](#)]
30. Smoláková, L.; Frolich, K.; Kocik, J.; Kikhtyanin, O.; Čapek, L. Surface Properties of Hydrotalcite-Based Zn(Mg)Al Oxides and Their Catalytic Activity in Aldol Condensation of Furfural with Acetone. *Indust. Eng. Chem. Res.* **2017**, *56*, 4638–4648. [[CrossRef](#)]
31. Kadlec, D.; Tišler, Z.; Velvarská, R.; Pelišková, L.; Akhmetzyanova, U. Comparison of the Properties and Catalytic Activity of Commercially and Laboratory Prepared Mg/Al Mixed Oxides in Aldol Condensation of Cyclohexanone with Furfural. *React. Kinet. Mech. Catal.* **2018**, *126*, 219–235. [[CrossRef](#)]



© 2019 by the authors. Licensee MDPI, Basel, Switzerland. This article is an open access article distributed under the terms and conditions of the Creative Commons Attribution (CC BY) license (<http://creativecommons.org/licenses/by/4.0/>).